International Journal of Systems Science and Applied Mathematics
2026, Vol. 11, No. 2, pp. 32–52
https://doi.org/10.11648/j.ijssam.20261102.12

SciencePG
Science Publishing Group

Research Article

Evaluation of CMIP6 Global Climate Models for Rainfall Simulation Across Agro-Ecological Zones of Ethiopia

Tewodros Solomon[1, *], **Yimer Assefa Yimam**[2]

[1]Department of Climate Change, Ethiopia Meteorology Institute, Bahir Dar, Ethiopia
[2]Ethiopia Meteorology Institute, Addis Ababa, Ethiopia

Abstract

Rainfall is one of the most critical climatic variables for investigating the impacts of climate change. Global Climate Models (GCMs) are widely used tools for examining changes in the climate system and projecting future climate scenarios. This study evaluated the performance of Coupled Model Intercomparison Project Phase 6 (CMIP6) Global Climate Models in simulating rainfall climatology over Ethiopia. Eight CMIP6 GCMs were assessed at daily, monthly, and annual timescales across five Agro-Ecological Zones (AEZs) of Ethiopia for the period 1995–2014, using station observations as reference data. Model performance was evaluated using Root Mean Square Error (RMSE), Percent Bias (PBIAS), and Pearson's correlation coefficient (r). Each model was ranked using the Comprehensive Rating Index (CRI). The results showed that model performance varied considerably for daily to annual rainfall totals across the AEZs, with both overestimation and underestimation observed. For daily rainfall, EC-Earth3-Veg performed best in tropical, subtropical, and temperate AEZs; MRI-ESM2-0 performed best in the desert AEZ; and MPI-ESM1-2-LR performed best in the alpine AEZ. BCC-CSM2-MR performed well across tropical, subtropical, temperate, and alpine AEZs, while MRI-ESM2-0 performed better in desert AEZs. For annual rainfall, MRI-ESM2-0 was superior in desert and tropical AEZs, BCC-CSM2-MR performed best in temperate and alpine AEZs, and EC-Earth3-Veg performed best in the subtropical AEZ. EC-Earth3 was the least effective at reproducing mean monthly rainfall. Overall, the models' performance was inconsistent across timescales and regions. Given the spatial and temporal variability in CMIP6 GCM performance, it is recommended that models be thoroughly evaluated and bias-corrected for specific locations and intended applications, particularly regarding their ability to simulate Ethiopia's diverse rainfall regimes.

Keywords

AEZs, CMIP6, GCMs, Rainfall, Model Performance Evaluation, Ethiopia

1. Introduction

Climate change is one of the most pressing issues threatening humanity in the twenty-first century. Extreme climatic events are becoming more frequent and intense, posing existential threats to agricultural livelihoods, water resources, human health, and economic development worldwide. Rainfall is one of the most critical climatic variables for assessing the impacts of climate change [5, 13]. Accelerated warming of the

*Correspondence: Tewodros Solomon (soloteddy77@gmail.com)

Received: 30 December 2025; **Accepted:** 18 May 2026; **Published:** 4 June 2026

Earth's surface has diverse consequences on the amount, distribution, and intensity of rainfall recorded in a given area [13, 23, 39]. Variations in rainfall distribution and intensity directly or indirectly trigger natural disasters such as floods and droughts [5, 13, 20, 25]. Continued and accelerated greenhouse gas emissions are projected to intensify climate change and variability, further increasing the frequency and magnitude of droughts and floods and exposing populations to greater water-related hazards [3, 32].

The impacts of hydrological and other climate-related risks are not uniform globally. Changes in rainfall intensity and frequency have particularly severe consequences for livelihoods in developing countries. In this regard, East Africa is among the region's most vulnerable to climate change and hydrological disasters due to high exposure and limited adaptive capacity [5, 13, 25, 39]. Ethiopia is also expected to face increasing climate-related disasters [33, 43]. Therefore, understanding historical and current rainfall patterns and associated disasters is essential for addressing future risks, enhancing adaptive capacity, and supporting consistent and reliable rainfall trend analysis and forecasting [43].

Global Climate Models (GCMs) have become the primary and most widely used tools for examining climate system changes driven by increased radiative forcing and for simulating historical and future climates [26, 38]. Since the 1950s, numerous GCMs have been developed by climate modeling centers worldwide [16]. Despite significant advancements, GCMs still suffer from limitations such as insufficient parameterization, coarse spatial resolution, and challenges in representing regional- and local-scale processes, particularly in areas with complex topography [11, 21]. These shortcomings contribute to substantial uncertainty in future climate projections, especially in topographically diverse regions [21].

To address these challenges, the Coupled Model Intercomparison Project (CMIP) provides a framework for coordinated climate model simulations. CMIP6 represents the latest phase, featuring improved model resolutions and a broader range of variables [18]. The ability of GCMs to accurately simulate current and past climates serves as a critical benchmark for the reliability of future projections. Consequently, thorough evaluation of GCM performance against high-quality observed data is essential [32]. Although several studies have evaluated CMIP5 models over Ethiopia and reported notable biases in simulating seasonal and annual rainfall [15, 28, 31], evaluations of CMIP6 models in the country remain limited [2, 14, 19].

Ethiopia is one of the most ecologically diverse countries in the world, characterized by its location in the tropics, extreme elevation gradients, and complex terrain [22, 29]. These features result in high spatial variability in climate and agro-ecology. Despite the importance of assessing CMIP6 model performance in reproducing daily, monthly, and annual rainfall across space and time, there is a lack of comprehensive national-scale studies that evaluate multiple CMIP6 models across Ethiopia's Agro-Ecological Zones (AEZs) with relevance to sectoral impact studies.

The present study aims to evaluate the performance of eight CMIP6 GCMs in simulating historical rainfall totals at daily, monthly, and annual timescales across all five AEZs of Ethiopia. This evaluation will assess the models' ability to represent spatiotemporal rainfall patterns before their application in future climate projections, thereby supporting the development of robust adaptation and climate-resilient strategies at the national level. The models were selected based on their strong performance in previous studies across Ethiopia, East Africa, and other regions [2], as well as their widespread use in earlier CMIP5 applications in Ethiopia [42]. Daily observed data were obtained from [24].

2. Materials and Methods

2.1. Description of Study Area

Ethiopia is located in the Horn of Africa between 3 °and 15 ° N latitude and 33 ° and 48 ° E longitude, covering an area of approximately 1.12 million km^2 [8]. The country is bordered by Eritrea to the north and northeast, Sudan and South Sudan to the west and northwest, Kenya to the south, and Somalia to the southeast [43].

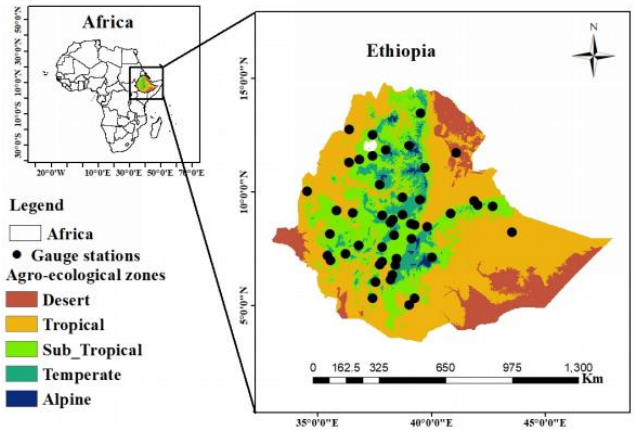

Figure 1. *Location of Ethiopia in Africa and the meteorological stations used in this study.*

Ethiopia is characterized by highly complex topography, with elevations ranging from 152 m below sea level in the Danakil Depression (northeastern part) to over 4,600 m above sea level (m.a.s.l.) at Mount Ras Dashen in the northern highlands [43]. The landscape includes rugged mountains, deep gorges, rolling plains, river valleys, and flat-topped plateaus [6]. Approximately 40% of the country lies above 1,500 m.a.s.l. and is classified as highland, while the remaining areas below 1,500 m.a.s.l. are considered lowland [9].

2.1.1. Traditional Agro-Ecological Zones (AEZs)

Ethiopia is traditionally divided into five Agro-Ecological

Zones (AEZs) Appendix 1: Bereha/Desert, Kolla/Tropical, Woina Dega/Subtropical, Dega/Temperate, and Wurch/Alpine. These zones are primarily defined by elevation as follows: Bereha/Desert (below 500 m.a.s.l), Kolla/Tropical: (500–1,500 m.a.s.l), WoinaDega/Subtropical (1,500–2,300 m.a.s.l, Dega/Temperate (2,300–3,200 m.a.s.l) and Wurch/Alpine (above 3,200 m.a.s.l). These classifications are based on altitude, annual rainfall, and temperature patterns [34].

2.1.2. Climate

The complex topography of Ethiopia creates diverse local climatic conditions, ranging from hot arid deserts in the northeast and southern lowlands to cold alpine climates in the Semien and Arsi-Bale mountain ranges [9]. Rainfall observation networks in the country are sparse and unevenly distributed, with many stations having short or discontinuous records of variable quality [12]. Ethiopia experiences three main seasons: Bega (dry season, October–January), Belg (short rainy season, February–May), and Kiremt (main rainy season, June–September). The duration and amount of rainfall in each season vary significantly across geographic regions [17].

2.2. Data Types and Sources

2.2.1. Ground-based (Observed) Rainfall Data

Daily observed rainfall data for the period 1995–2014 were obtained from 47 meteorological stations Appendix 1, managed by the Ethiopian Meteorology Institute (EMI). These stations were selected based on record length and data completeness. Of the 47 stations, 28 are located in the Woina Dega/Subtropical, 9 in Kolla/Tropical, 8 in Dega/Temperate, and one each in Wurch/Alpine and Bereha/Desert AEZs.

Stations with missing data less than 25% were selected, which is acceptable in data-scarce regions such as Ethiopia. Missing values were filled using the Multivariate Imputation by Chained Equations (MICE) package in R. Quality control was performed using the RClimDex package [44], where negative values were replaced with data from the nearest station, and outliers were treated following World Meteorological Organization (WMO) guidelines [40]. Detailed procedures for data processing and gap filling are described in [43]. Station locations and characteristics are provided in Appendix 1.

2.2.2. CMIP6 GCMs Model Data

The performance of eight CMIP6 Global Climate Models (GCMs) developed by various institutions was evaluated in this study (Table 1). Historical simulations for the period 1995–2014 were used. Model outputs were downloaded from the Earth System Grid Federation (ESGF) archive using the following criteria: Variable = precipitation, Frequency = day, Experiment ID = historical, and the respective Source IDs.

Table 1. *List of CMIP6 GCMs used in this study and their characteristics.*

Number	CMIP6 model	Institute	Country	Resolution	Variant label
1	ACCESS-ESM1-5	Australian Community Climate and Earth System Simulator	Australia	1.9 °×1.2 °	r1i1p1f1
2	BCC-CSM2-MR	Beijing Climate Center (BCC)	China	1.1 °×1.1 °	r1i1p1f1
3	CNRM-CM6-1	Recherch é M é t éorologiques	France	1.4 × 1.4◦	r1i1p1f2
4	EC-Earth3	EC-Earth-Consortium	Sweden	0.7 ° × 0.7 °	r1i1p1f1
5	EC-Earth3-veg	EC-Earth-Consortium	Sweden	0.7 ° × 0.7 °	r1i1p1f1
6	MPI-ESM1-2-LR	Max-Planck-Institute f ür Meteorology	Germany	1.9 °×1.9 °	r1i1p1f1
7	MRI-ESM2-0	Meteorological Research Institute	Japan	1.1 °×1.1 °	r1i1p1f1
8	GFDL-ESM4	Geophysical fluid dynamics laboratory	USA	1.25 °×1.00 °	r1i1p1f1

The GCMs were selected based on daily data availability and demonstrated good performance in previous studies over Ethiopia [2], East Africa [24], and other regions [27], as well as their widespread use in CMIP5 applications in Ethiopia [42].

GCM rainfall data were extracted at each station location using the CMhyd tool [22] to enable direct comparison with observed data.

2.3. Methods of Analysis

2.3.1. Research Framework

The overall research framework of this study is presented in Figure 2. CMIP6 GCM outputs were first extracted for the 47 meteorological stations. Point-scale observed data were

then converted to a real average where appropriate. Model performance was evaluated separately for each of the five AEZs (desert, tropical, subtropical, temperate, and alpine) over the period 1995–2014. All data processing and statistical analyses were conducted in R software.

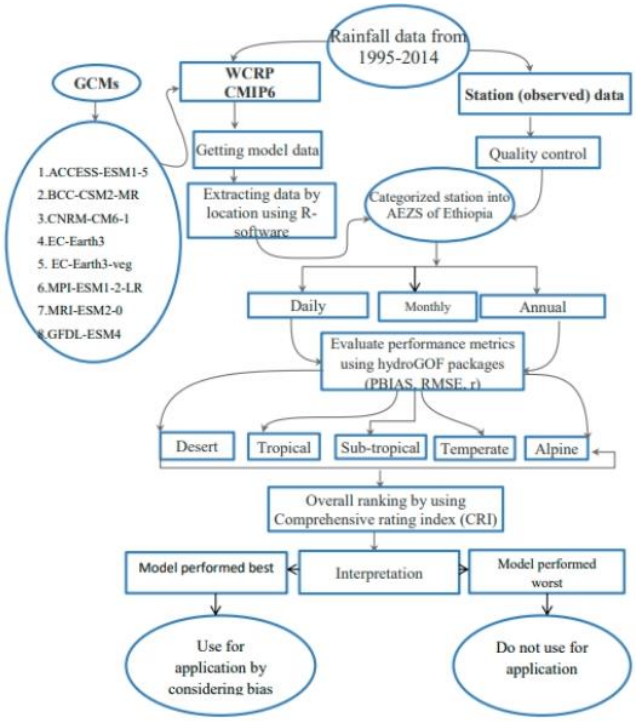

Figure 2. *Research framework of the study.*

2.3.2. Performance Metrics for Evaluation of CMIP6 GCMs

Model performance was assessed using three statistical metrics: Percent Bias (PBIAS), Root Mean Square Error (RMSE), and Pearson's correlation coefficient (r). These metrics have been widely used in similar studies in Ethiopia and elsewhere [10, 22, 25, 41].

1) Percent Bias (PBIAS) measures the tendency of the model to over- or underestimate observed data. Values closer to zero indicate better performance [7].
2) Root Mean Square Error (RMSE) quantifies the magnitude of errors between simulated and observed values (lower values are better) [1].
3) Pearson's correlation coefficient (r) assesses the linear agreement between simulated and observed data (values closer to 1 are better) [12].

The formulas for these metrics are as follows:

$$PBIAS\ (\%) = \frac{\sum_{i=1}^{n}(S_i - O_i)}{\sum_{i=1}^{n} O_i} \times 100 \quad (1)$$

$$RMSE = \sqrt{\frac{1}{n}\sum_{i=1}^{n}(S_i - O_i)^2} \quad (2)$$

$$r = \frac{\sum_{i=1}^{N}(O_i - \dot{O})(S_i - \dot{S})}{\sqrt{\sum_{i=1}^{N}(O_i - \dot{O})^2 \sum_{i=1}^{N}(S_i - \dot{S})^2}} \quad (3)$$

Where O_i and S_i are observed and simulated rainfall, rainfall, $\dot{O}$ and $\dot{S}$ is are their respective means, and N is the number of data pairs.

2.3.3. Comprehensive Rating Index (CRI)

The Comprehensive Rating Index (CRI) was used to rank the overall performance of the GCMs by integrating the three metrics. The CRI has been widely applied in recent CMIP6 evaluation studies [22]. The CRI is calculated as:

$$CRI = \frac{1}{n}\sum_{i=1}^{n}\left(1 - \frac{R_i - 1}{m - 1}\right) \quad (4)$$

Where n is the number of statistical metrics, m is the number of GCMs, and R_i is the rank of a model for each metric. A CRI value closer to 1 indicates better model performance.

2.3.4. Performance Evaluation Using Graphical Techniques

Graphical methods were employed to visually assess model performance. Line graphs were used to compare mean observed and simulated rainfall at daily, monthly, and annual timescales across the AEZs. These techniques complement statistical metrics by revealing patterns, distributions, and seasonal biases [7, 30, 36].

3. Results and Discussions

3.1. Performance Evaluation of CMIP6 GCMs for Daily Rainfall

The performance metrics and rankings of the eight CMIP6 GCMs for daily rainfall simulation across the five Agro-Ecological Zones (AEZs) of Ethiopia (1995–2014) are presented in Table 2. In the desert AEZ, MRI-ESM2-0 was the best-performing model, followed by EC-Earth3-Veg and BCC-CSM2-MR. CNRM-CM6-1 and GFDL-ESM4 performed poorest. Most models underestimated daily rainfall in this zone (positive PBIAS), with GFDL-ESM4 showing the largest overestimation (128.8%).

In the tropical AEZ, EC-Earth3-Veg, MPI-ESM1-2-LR, and ACCESS-ESM1-5 ranked first, second, and third, respectively. BCC-CSM2-MR and CNRM-CM6-1 performed worst. Four models overestimated and four underestimated daily rainfalls. The best model (EC-Earth3-Veg) underestimated rainfall by 11.4%. In the subtropical AEZ, EC-Earth3-Veg, MPI-ESM1-2-LR, and MRI-ESM2-0 were the top three models, while BCC-CSM2-MR and CNRM-CM6-1 ranked lowest. EC-Earth3-Veg underestimated daily rainfall by 1.6%.

In the temperate AEZ, EC-Earth3-Veg was the best-performing model, while ACCESS-ESM1-5 performed worst.

Most models overestimated daily rainfall. EC-Earth3-Veg overestimated by 9.2%. In the alpine AEZ, MPI-ESM1-2-LR performed best, followed by ACCESS-ESM1-5. Most models underestimated daily rainfall, although MRI-ESM2-0, GFDL-ESM4, and EC-Earth3-Veg overestimated it. MPI-ESM1-2-LR underestimated rainfall by 24.6%.

No single model outperformed all others across AEZs, demonstrating the value of the Comprehensive Rating Index (CRI) for integrated evaluation. Overall, EC-Earth3-Veg performed best in tropical, subtropical, and temperate AEZs, MRI-ESM2-0 in the desert AEZ, and MPI-ESM1-2-LR in the alpine AEZ. Model performance was generally better in lowland (desert and tropical) than in highland (temperate and alpine) AEZs, highlighting the persistent challenge of complex topography in climate modeling [4].

Table 2. *Performance of CMIP6 GCMs for simulating daily rainfall over AEZs of Ethiopia (1995–2014).*

AEZs	CMIP6 Models	Continuous Statistical Metrics			CRI	Rank
		RMSE	PBIAS	r		
Desert	ACCESS-ESM-1-5	4.49	64.10	0.05	0.42	5
	BCC-CSM-2-MR	4.00	-16.40	0.04	0.58	3
	CNRM-CM6-1	4.07	48.50	0.00	0.21	7
	EC-Earth3	3.43	91.90	0.03	0.46	4
	EC-Earth3-veg	3.82	11.10	0.04	0.71	2
	GFDL-ESM4	5.63	-128.80	0.01	0.08	8
	MPI-ESM1-2-LR	3.86	47.90	0.01	0.42	5
	MRI-ESM2-0	3.81	3.00	0.04	0.79	1
Tropical	ACCESS-ESM-1-5	4.06	-30.80	0.28	0.54	3
	BCC-CSM-2-MR	5.49	-30.30	0.20	0.29	7
	CNRM-CM6-1	3.76	58.40	0.12	0.29	7
	EC-Earth3	3.80	91.60	0.28	0.46	4
	EC-Earth3-veg	3.51	11.40	0.23	0.63	1
	GFDL-ESM4	4.55	-10.50	0.19	0.38	6
	MPI-ESM1-2-LR	3.28	38.40	0.27	0.58	2
	MRI-ESM2-0	4.06	-6.20	0.10	0.42	5
Sub-tropical	ACCESS-ESM-1-5	5.34	37.10	0.41	0.29	6
	BCC-CSM-2-MR	5.74	-19.80	0.32	0.25	7
	CNRM-CM6-1	4.20	46.40	0.19	0.25	7
	EC-Earth3	4.31	90.70	0.55	0.42	4
	EC-Earth3-veg	3.45	1.60	0.49	0.79	1
	GFDL-ESM4	4.69	-3.50	0.35	0.42	4
	MPI-ESM1-2-LR	3.26	32.10	0.47	0.67	2
	MRI-ESM2-0	4.27	-32.10	0.39	0.46	3
Temperate	ACCESS-ESM-1-5	5.66	-50.10	0.38	0.21	8
	BCC-CSM-2-MR	5.73	1.00	0.28	0.33	7
	CNRM-CM6-1	4.85	-17.30	0.28	0.38	5
	EC-Earth3	4.77	89.60	0.53	0.50	3
	EC-Earth3-veg	4.26	-9.20	0.47	0.75	1

AEZs	CMIP6 Models	Continuous Statistical Metrics			CRI	Rank
		RMSE	PBIAS	r		
Alpine	GFDL-ESM4	5.17	-3.90	0.33	0.38	5
	MPI-ESM1-2-LR	3.96	30.10	0.42	0.58	2
	MRI-ESM2-0	5.13	-35.00	0.44	0.42	4
	ACCESS-ESM-1-5	7.29	23.30	0.28	0.54	2
	BCC-CSM-2-MR	7.76	9.80	0.18	0.42	4
	CNRM-CM6-1	7.51	36.60	0.07	0.29	6
	EC-Earth3	6.56	86.00	0.31	0.50	3
	EC-Earth3-veg	7.67	-48.30	0.29	0.29	6
	GFDL-ESM4	7.81	-15.60	0.17	0.29	6
	MPI-ESM1-2-LR	6.28	24.60	0.33	0.75	1
	MRI-ESM2-0	7.57	-39.00	0.30	0.42	4

Ranks are based on the CRI; rank 1 indicates the best-performing model and rank 8 the poorest. The Taylor diagram [37] in Figure 3, summarizes the performance of CMIP6 GCMs in terms of correlation coefficient, standard deviation, and centered root mean square error across the agro-ecological zones (AEZs) of Ethiopia. The best-ranked models generally exhibited higher correlations with observations. Standard deviations varied considerably among the models, with some closely matching the observed variability (e.g., ACCESS-ESM1-5 in the desert zone and EC-Earth3-Veg in the tropical zone).

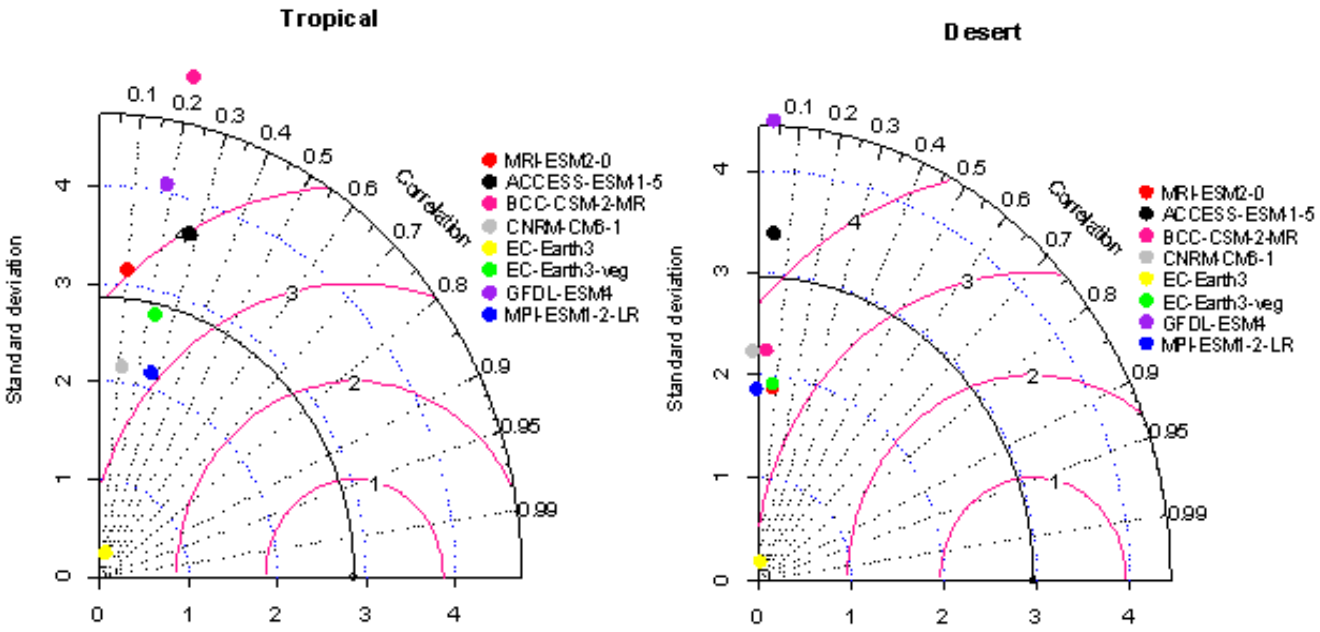

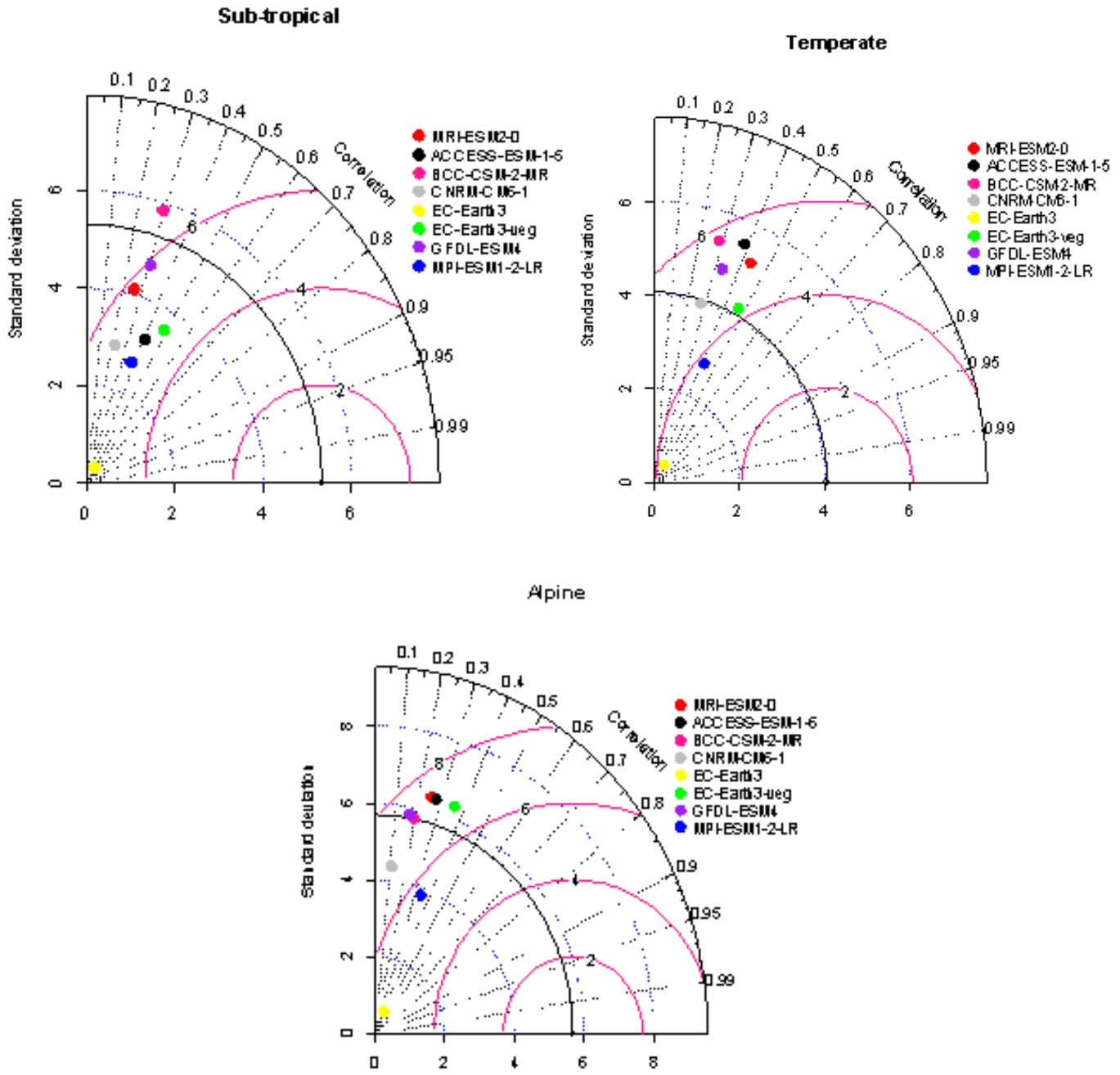

Figure 3. *Taylor diagram showing the performance of CMIP6 GCMs for daily rainfall against observations across AEZs of Ethiopia (1995–2014), the black dot on the solid line represents the observed data.*

3.2. Performance Evaluation of CMIP6 GCMs for Monthly Rainfall

Performance metrics and rankings for monthly rainfall are shown in Table 3. The Tropical, Sub-tropical, and Temperate AEZs generally exhibited relatively better model performance, characterized by higher correlation coefficients and lower RMSE values compared to the Desert and Alpine AEZs. This suggests that models are more capable of reproducing rainfall variability in regions dominated by relatively organized monsoonal rainfall systems than in areas strongly influenced by localized topographic and convective processes.

In the Desert AEZ, the performance of most models was relatively weak, reflecting the difficulty of simulating rainfall in arid environments where precipitation is sparse, highly variable, and dominated by isolated convective events. Among the models, EC-Earth3-veg and MRI-ESM2-0 achieved the highest CRI values (0.75) and ranked first, indicating comparatively better performance. These models also exhibited relatively lower RMSE and moderate positive correlations. In contrast, ACCESS-ESM-1-5 showed the poorest performance, with extremely high negative PBIAS (-178.40%) and low CRI (0.13), indicating substantial underestimation of rainfall. The

poor performance in the Desert AEZ may be associated with limitations in representing localized atmospheric dynamics and land–atmosphere interactions under dry climatic conditions.

The Tropical AEZ showed improved model skill relative to the Desert region. BCC-CSM-2-MR ranked first with a CRI value of 0.71, supported by relatively low RMSE (53.03 mm), small negative bias (-30.30%), and strong correlation (r = 0.74). MPI-ESM1-2-LR also demonstrated strong performance with high correlation (0.70) and low RMSE (48.20 mm). However, EC-Earth3 and CNRM-CM6-1 showed lower CRI values due to large positive rainfall biases exceeding 50%, indicating overestimation of precipitation amounts. The improved performance in the Tropical AEZ likely reflects the stronger influence of large-scale circulation systems, such as the Intertropical Convergence Zone (ITCZ), which are generally better represented in global climate models.

The Sub-tropical AEZ exhibited the best overall model performance among all AEZs, with relatively high correlation coefficients ranging from 0.67 to 0.85. BCC-CSM-2-MR again emerged as the best-performing model with the highest CRI (0.79), followed by EC-Earth3-veg and MPI-ESM1-2-LR (CRI = 0.63). These models successfully captured monthly rainfall variability while maintaining lower RMSE and moderate biases. Conversely, ACCESS-ESM-1-5 and CNRM-CM6-1 performed poorly due to high RMSE values and substantial rainfall biases. The better model performance in this AEZ may be attributed to the relatively homogeneous rainfall distribution and stronger synoptic-scale controls.

Similarly, in the Temperate AEZ, BCC-CSM-2-MR demonstrated superior performance with the highest CRI value (0.83), the lowest RMSE (46.67 mm), near-zero bias (0.90%), and a strong correlation coefficient (0.85). MPI-ESM1-2-LR and GFDL-ESM4 also showed satisfactory performance. The consistent skill of BCC-CSM-2-MR across Tropical, Sub-tropical, and Temperate AEZs indicates its strong capability in representing Ethiopia's rainfall climatology. However, EC-Earth3 and ACCESS-ESM-1-5 displayed relatively poor performance due to large positive and negative biases, respectively. The strong performance in the Temperate AEZ may be related to the dominance of seasonal rainfall systems that are more predictable at the large scale.

In contrast, the Alpine AEZ recorded the weakest model performance overall, characterized by very high RMSE values (144–182 mm) and weak correlations (0.03–0.33). Although ACCESS-ESM-1-5 and BCC-CSM-2-MR achieved the highest CRI values (0.67), the overall skill remained limited due to large errors and weak representation of rainfall variability. The poor performance in the Alpine region is likely associated with Ethiopia's complex mountainous topography, which strongly influences orographic rainfall processes that are difficult for coarse-resolution GCMs to capture accurately. Similar findings have been reported in previous studies over East Africa and the Ethiopian Highlands, where climate models often struggle to simulate localized precipitation influenced by elevation gradients and terrain-induced convection.

Across all AEZs, BCC-CSM-2-MR consistently ranked among the top-performing models, indicating its robustness in simulating Ethiopian rainfall patterns. MPI-ESM1-2-LR, GFDL-ESM4, and EC-Earth3-veg also showed reasonable performance in several AEZs. Conversely, ACCESS-ESM-1-5 and CNRM-CM6-1 frequently exhibited poor performance due to large rainfall biases and higher RMSE values. The variation in model performance highlights the importance of regional evaluation before selecting GCMs for climate change impact studies, hydrological modeling, and agricultural applications in Ethiopia.

Table 3. *Performance of CMIP6 GCMs for simulating monthly rainfall over AEZs of Ethiopia (1995–2014).*

AEZs	CMIP6 Models	Continuous statistical metrics			CRI	Rank
		RMSE	PBIAS	r		
Desert	ACCESS-ESM-1-5	55.33	-178.40	0.40	0.13	8
	BCC-CSM-2-MR	31.44	-16.40	0.05	0.46	4
	CNRM-CM6-1	38.83	48.50	-0.04	0.21	7
	EC-Earth3	30.08	91.80	0.37	0.63	3
	EC-Earth3-veg	29.98	11.10	0.33	0.75	1
	GFDL-ESM4	50.78	-128.60	0.31	0.25	6
	MPI-ESM1-2-LR	37.11	48.00	0.00	0.33	5
	MRI-ESM2-0	30.18	3.00	0.36	0.75	1
Tropical	ACCESS-ESM-1-5	73.12	-30.80	0.63	0.33	6
	BCC-CSM-2-MR	53.03	-30.30	0.74	0.71	1

AEZs	CMIP6 Models	Continuous statistical metrics			CRI	Rank
		RMSE	PBIAS	r		
Sub-tropical	CNRM-CM6-1	70.16	58.40	0.36	0.21	7
	EC-Earth3	89.53	91.60	0.65	0.21	7
	EC-Earth3-veg	57.18	11.40	0.55	0.50	4
	GFDL-ESM4	57.26	-10.80	0.61	0.54	3
	MPI-ESM1-2-LR	48.20	38.30	0.70	0.63	2
	MRI-ESM2-0	70.76	-6.20	0.23	0.38	5
	ACCESS-ESM-1-5	116.04	-58.90	0.67	0.08	8
	BCC-CSM-2-MR	52.14	-19.80	0.85	0.79	1
Temperate	CNRM-CM6-1	85.53	46.40	0.42	0.17	7
	EC-Earth3	115.35	90.70	0.85	0.33	6
	EC-Earth3-veg	60.61	1.60	0.77	0.63	2
	GFDL-ESM4	58.01	-3.50	0.75	0.58	4
	MPI-ESM1-2-LR	52.91	32.10	0.84	0.63	2
	MRI-ESM2-0	68.50	-32.10	0.73	0.38	5
	ACCESS-ESM-1-5	108.05	-50.10	0.69	0.13	8
	BCC-CSM-2-MR	46.67	0.90	0.85	0.83	1
Alpine	CNRM-CM6-1	74.66	17.30	0.61	0.29	6
	EC-Earth3	116.44	89.60	0.89	0.29	6
	EC-Earth3-veg	67.02	-9.30	0.79	0.50	4
	GFDL-ESM4	59.35	-3.90	0.77	0.54	3
	MPI-ESM1-2-LR	58.52	30.00	0.82	0.58	2
	MRI-ESM2-0	75.12	-35.00	0.81	0.33	5
	ACCESS-ESM-1-5	150.66	-18.60	0.33	0.67	1
	BCC-CSM-2-MR	144.58	18.10	0.14	0.67	1
	CNRM-CM6-1	145.42	42.30	0.13	0.38	5
	EC-Earth3	152.26	87.30	0.26	0.38	5
	EC-Earth3-veg	172.89	-34.90	0.22	0.33	7
	GFDL-ESM4	154.37	-5.00	0.04	0.42	4
	MPI-ESM1-2-LR	147.56	31.40	0.15	0.50	3
	MRI-ESM2-0	182.12	-26.50	0.03	0.17	8

Figure 4 illustrates the comparison between observed mean monthly rainfall and rainfall simulated by CMIP6 GCMs across the Agro-Ecological Zones (AEZs) of Ethiopia during the period 1995–2014. The results indicate considerable variability in model performance among the AEZs and across different seasons. Overall, some models demonstrated relatively good capability in reproducing the seasonal rainfall cycle, while others showed substantial overestimation or underestimation of rainfall amounts.

Over the Desert AEZ, EC-Earth3-veg and GFDL-ESM4 relatively better represented the long-term mean rainfall during the wet months (June, July, August, and September). In contrast, MPI-ESM1-2-LR and CNRM-CM6-1 showed comparatively better performance in simulating rainfall during the

dry months (October, November, December, and January). However, ACCESS-ESM1-5 and GFDL-ESM4 performed poorly in capturing the wet and dry season rainfall patterns, respectively. The difficulty in reproducing rainfall over arid regions may be associated with the sporadic and localized nature of precipitation in desert environments.

In the Tropical AEZ, GFDL-ESM4 showed the closest agreement with observed mean monthly rainfall, indicating relatively strong performance in reproducing the seasonal rainfall distribution. Similarly, EC-Earth3-veg also demonstrated good capability in simulating monthly rainfall, except during April and May, where noticeable deviations from observations were observed (Figure 4). Conversely, EC-Earth3 exhibited the weakest performance, with substantial discrepancies from observed rainfall throughout the study period.

Over the Sub-tropical AEZ, GFDL-ESM4, EC-Earth3-veg, and BCC-CSM2-MR were relatively successful in capturing the observed mean monthly rainfall pattern. These models reproduced the seasonal rainfall cycle reasonably well, particularly during the main rainy season. In contrast, CNRM-CM6-1, EC-Earth3, and ACCESS-ESM1-5 showed poor performance, especially during the wet months (June–September), where they either overestimated or underestimated rainfall considerably (Figure 4).

Similarly, in the Temperate AEZ, the simulated rainfall from GFDL-ESM4, EC-Earth3-veg, and BCC-CSM2-MR closely matched the observed rainfall distribution. These models captured both the magnitude and timing of seasonal rainfall more effectively than the other models. However, EC-Earth3 and ACCESS-ESM1-5 showed large deviations from observations. In particular, EC-Earth3 substantially underestimated mean monthly rainfall across almost all months in the Temperate AEZ (Figure 4).

In the Alpine AEZ, EC-Earth3-veg and MRI-ESM2-0 showed relatively good skill in reproducing rainfall during June and July, which are typically peak rainfall months. On the other hand, GFDL-ESM4 performed comparatively better during the dry season months (October–January). Nevertheless, GFDL-ESM4 tended to overestimate rainfall during the dry season while underestimating rainfall during the wet season (June–September).

Similar findings were reported by [35], who noted that many climate models overestimate rainfall during April–September over the Upper Blue Nile Basin in northwestern Ethiopia. EC-Earth3 was identified as the poorest-performing model in the Alpine AEZ, as it consistently underestimated rainfall throughout the year.

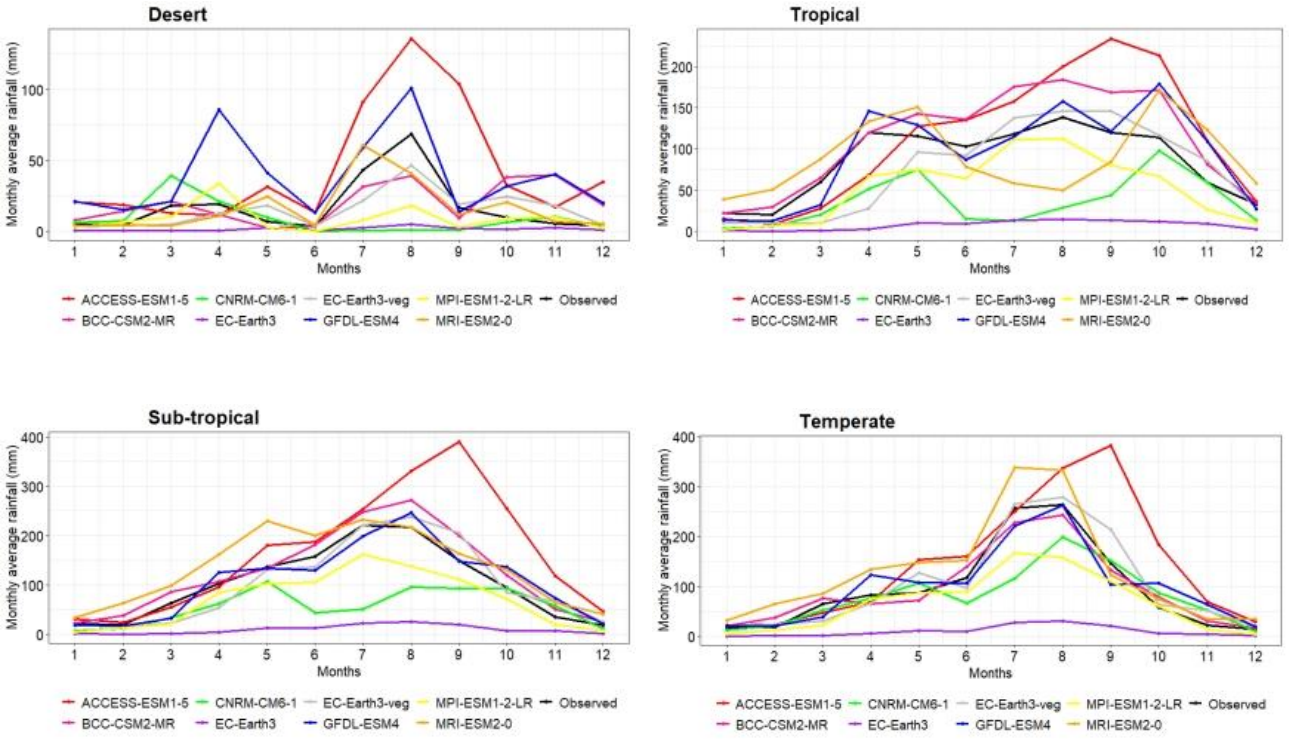

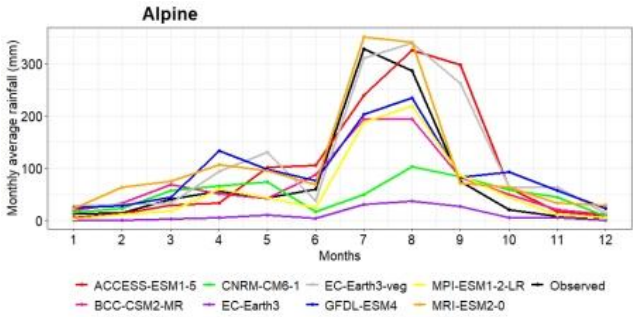

Figure 4. *Line graphs comparing mean monthly observed and simulated rainfall by CMIP6 GCMs across AEZs of Ethiopia (1995–2014).*

Figure 5 presents the Taylor diagrams used to evaluate the performance of CMIP6 Global Climate Models (GCMs) in simulating monthly rainfall across the Agro-Ecological Zones (AEZs) of Ethiopia during the period 1995–2014. The Taylor diagram provides a comprehensive statistical comparison between observed and simulated rainfall by simultaneously illustrating the correlation coefficient, standard deviation, and centered root mean square error (RMSE). In the diagrams, models positioned closer to the reference observation point indicate better agreement with observed rainfall characteristics.

The results revealed substantial spatial variability in model performance across the AEZs of Ethiopia. In general, the Tropical, Sub-tropical, and Temperate AEZs exhibited relatively stronger model performance, whereas the Desert and Alpine AEZs showed comparatively weaker performance and larger model dispersion. This indicates that the ability of CMIP6 GCMs to reproduce monthly rainfall is highly dependent on regional climatic characteristics and topographic complexity.

In the Desert AEZ, most models showed relatively low correlations with observations and moderate deviations in standard deviation. EC-Earth3-veg and MRI-ESM2-0 were positioned comparatively closer to the reference point, indicating relatively better skill in reproducing rainfall variability over the arid region. However, several models, including ACCESS-ESM1-5 and GFDL-ESM4, were located farther from the observation point, reflecting weaker correlations and higher simulation errors. The relatively poor performance of models in the Desert AEZ may be associated with the highly erratic and localized nature of rainfall in arid environments, which is difficult for coarse-resolution GCMs to represent accurately.

The Tropical AEZ demonstrated improved model performance compared to the Desert region. Most models exhibited moderate to high correlations with observations and relatively closer standard deviations to the observed rainfall. BCC-CSM2-MR, MPI-ESM1-2-LR, and GFDL-ESM4 appeared closer to the observation reference, suggesting stronger skill in capturing both rainfall variability and seasonal patterns. In contrast, EC-Earth3 and CNRM-CM6-1 showed relatively larger deviations from the reference point, indicating weaker agreement with observed rainfall characteristics. The relatively better performance in the Tropical AEZ may be linked to the dominance of large-scale atmospheric circulation systems, such as the Intertropical Convergence Zone (ITCZ), which are generally better represented in climate models.

Similarly, the Sub-tropical AEZ showed relatively strong model performance, with several models clustered near the observation point. BCC-CSM2-MR, EC-Earth3-veg, and MPI-ESM1-2-LR demonstrated high correlations and standard deviations close to observations, indicating good capability in reproducing monthly rainfall variability. However, ACCESS-ESM1-5 and EC-Earth3 displayed larger deviations and weaker correlations, suggesting limited performance in capturing rainfall dynamics over the region. The better agreement observed in the Sub-tropical AEZ could be attributed to relatively organized seasonal rainfall systems and less localized rainfall variability compared to mountainous regions.

In the Temperate AEZ, the Taylor diagram indicated that BCC-CSM2-MR, GFDL-ESM4, and EC-Earth3-veg performed relatively well, as they were located nearer to the observation reference point with high correlation coefficients and moderate standard deviation differences. Conversely, ACCESS-ESM1-5 and EC-Earth3 showed larger distances from the observation point, indicating greater simulation errors and weaker representation of rainfall variability. The relatively high model skill observed in the Temperate AEZ suggests that the models were more successful in capturing the dominant seasonal rainfall characteristics in this region.

The Alpine AEZ exhibited the weakest model performance among all AEZs. Most models showed low correlation coefficients and large standard deviations relative to observations, resulting in substantial scatter in the Taylor diagram. Although ACCESS-ESM1-5 and BCC-CSM2-MR showed relatively better positioning compared to other models, the overall agreement with observations remained weak. The large spread among models in the Alpine AEZ indicates considerable uncertainty in simulating rainfall over high-altitude regions. This may be attributed to the complex topography of the Ethiopian Highlands, where localized convective processes and orographic effects strongly influence rainfall distribution. Such fine-scale processes are often inadequately represented in coarse-resolution GCMs.

Overall, the Taylor diagram analysis confirms that no single CMIP6 model consistently outperformed others across all AEZs of Ethiopia. Nevertheless, BCC-CSM2-MR, EC-

Earth3-veg, GFDL-ESM4, and MPI-ESM1-2-LR generally demonstrated comparatively better performance in reproducing monthly rainfall characteristics. In contrast, EC-Earth3 and ACCESS-ESM1-5 consistently exhibited weaker performance across most AEZs. These findings are consistent with previous studies conducted in Ethiopia and East Africa, which reported substantial regional variability in CMIP6 model performance due to differences in topography, atmospheric circulation, and rainfall-generating mechanisms.

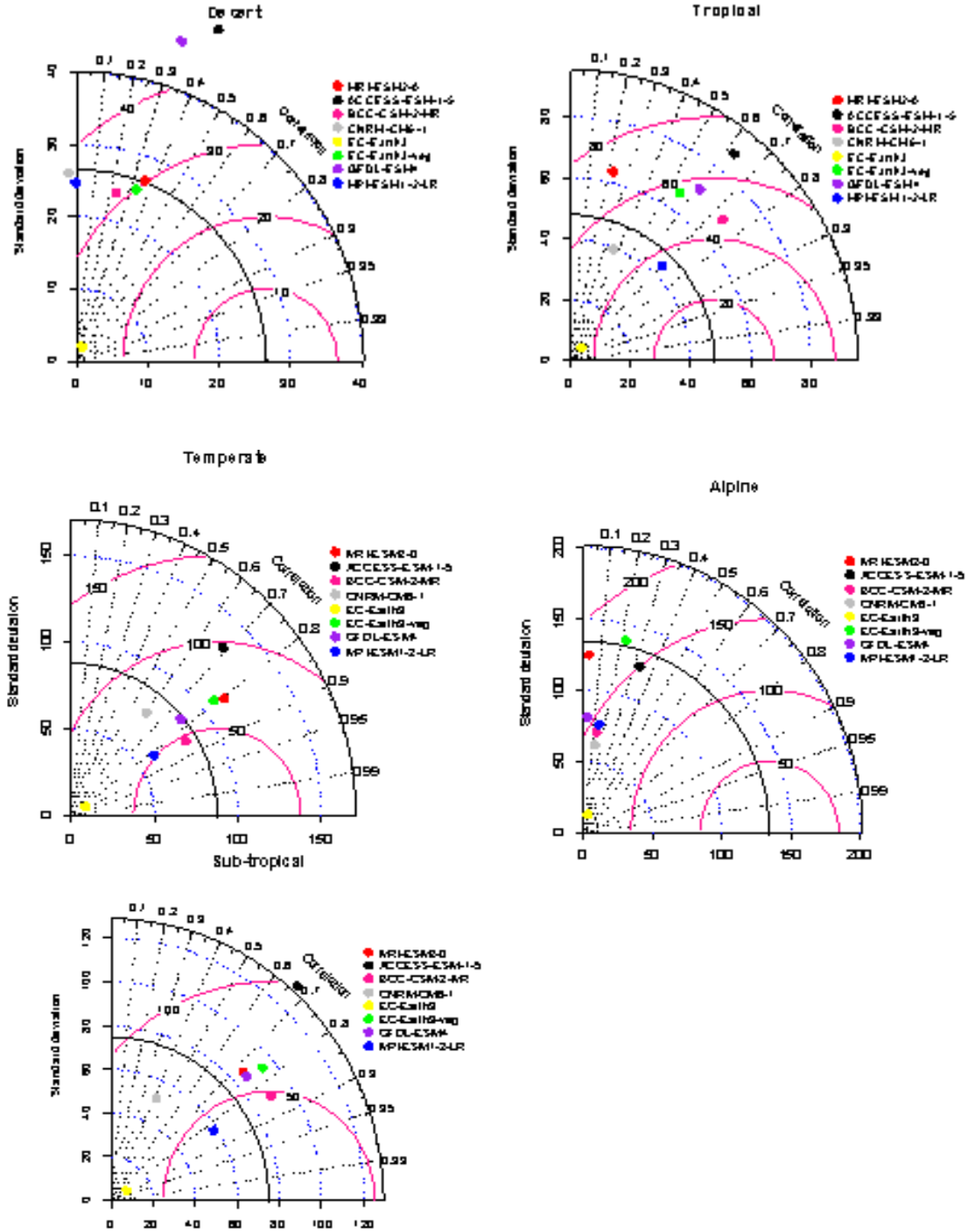

Figure 5. Taylor diagram of CMIP6 GCMs for monthly rainfall against observations across AEZs of Ethiopia (1995–2014).

3.3. Performance Evaluation of CMIP6 GCMs for Annual Rainfall

Table 4 presents the evaluation of CMIP6 Global Climate Models (GCMs) in simulating annual rainfall across the Agro-Ecological Zones (AEZs) of Ethiopia during the historical period 1995–2014. The performance assessment was conducted using Root Mean Square Error (RMSE), Percent Bias (PBIAS), correlation coefficient (r), and Composite Rating Index (CRI). The results demonstrate considerable spatial variability in model performance across the AEZs, reflecting the complex climatic and topographic characteristics of Ethiopia.

In the Desert AEZ, most models showed relatively weak performance due to the highly variable and sporadic nature of rainfall in arid regions. MRI-ESM2-0 emerged as the best-performing model with the highest CRI value (0.83), the lowest RMSE (79.64 mm), and a relatively small bias (3.10%), indicating strong agreement with observed annual rainfall. BCC-CSM-2-MR also showed good performance with low RMSE and moderate correlation. In contrast, ACCESS-ESM1-5 and GFDL-ESM4 exhibited very poor performance, characterized by extremely large negative biases and weak negative correlations, suggesting substantial underestimation of annual rainfall. The poor performance of some models in the Desert AEZ may be associated with difficulties in representing localized convective rainfall and land–atmosphere interactions in dry environments.

In the Tropical AEZ, model performance improved compared to the Desert region. GFDL-ESM4 and EC-Earth3-veg demonstrated relatively good performance with lower RMSE values and smaller rainfall biases. MRI-ESM2-0 achieved the highest CRI ranking despite having a relatively low correlation coefficient, mainly due to its lower RMSE and smaller bias. On the other hand, EC-Earth3 and MPI-ESM1-2-LR showed weaker performance, with large RMSE values and poor correlations. EC-Earth3 particularly overestimated annual rainfall by about 91.60%, indicating substantial systematic error in rainfall simulation. The relatively better performance in the Tropical AEZ may be related to the stronger influence of large-scale atmospheric circulation systems, such as the Intertropical Convergence Zone (ITCZ), which are more effectively represented in GCMs.

The Sub-tropical AEZ exhibited relatively strong model performance overall. EC-Earth3-veg was identified as the best-performing model with the highest CRI value (0.79), low RMSE (241.70 mm), and very small bias (1.60%). GFDL-ESM4 also demonstrated strong performance with the lowest RMSE (182.45 mm) and minimal bias (-3.50%). In contrast, EC-Earth3 and ACCESS-ESM1-5 showed the weakest performance due to extremely high RMSE values and substantial rainfall biases. The relatively good performance of EC-Earth3-veg and GFDL-ESM4 suggests their better capability in reproducing annual rainfall variability over regions dominated by seasonal monsoonal rainfall systems.

Similarly, in the Temperate AEZ, BCC-CSM-2-MR showed the best overall performance with the highest CRI value (0.79), the lowest RMSE (146.43 mm), and nearly unbiased rainfall simulation (0.90%). EC-Earth3-veg and CNRM-CM6-1 also performed reasonably well with moderate RMSE values and positive correlations. Conversely, EC-Earth3 recorded the poorest performance, characterized by extremely high RMSE (1033.63 mm) and substantial overestimation of rainfall (89.60%). ACCESS-ESM1-5 and MRI-ESM2-0 also showed weaker performance due to large negative rainfall biases. The stronger performance in the Temperate AEZ may indicate that some models are better able to simulate rainfall regimes influenced by relatively stable seasonal atmospheric circulation.

In the Alpine AEZ, BCC-CSM-2-MR was the best-performing model with the highest CRI value (0.83), relatively low RMSE (151.93 mm), and moderate positive correlation (0.49). ACCESS-ESM1-5 and GFDL-ESM4 also showed relatively good performance compared to other models. However, EC-Earth3 again showed poor performance with very high RMSE and large positive rainfall bias. Although EC-Earth3-veg exhibited the highest correlation coefficient (0.62), its large negative bias and high RMSE reduced its overall ranking. The generally weaker model performance in the Alpine AEZ may be associated with Ethiopia's complex mountainous topography, where localized orographic rainfall processes are difficult for coarse-resolution GCMs to accurately reproduce.

Overall, the results indicate that no single CMIP6 model consistently outperformed all others across every AEZ. However, BCC-CSM-2-MR, EC-Earth3-veg, GFDL-ESM4, and MRI-ESM2-0 demonstrated relatively reliable performance across multiple AEZs. In contrast, EC-Earth3 consistently exhibited poor performance due to high RMSE values, large rainfall biases, and weak correlations across most AEZs. ACCESS-ESM1-5 also showed substantial deficiencies in simulating annual rainfall, particularly in the Desert and Sub-tropical AEZs.

Table 4. *Performance of CMIP6 GCMs for simulating annual rainfall over AEZs of Ethiopia (1995–2014).*

AEZs	CMIP6 Models	Continuous statistical metrics			CRI	Rank
		RMSE	PBIAS	r		
Desert	ACCESS-ESM-1-5	395.63	-178.40	-0.09	0.04	8

AEZs	CMIP6 Models	Continuous statistical metrics			CRI	Rank
		RMSE	PBIAS	r		
Tropical	BCC-CSM-2-MR	86.36	-16.40	0.19	0.67	2
	CNRM-CM6-1	122.82	48.60	0.58	0.58	3
	EC-Earth3	196.44	91.90	-0.05	0.29	6
	EC-Earth3-veg	120.08	11.20	-0.08	0.54	4
	GFDL-ESM4	303.17	-128.50	-0.14	0.08	7
	MPI-ESM1-2-LR	133.78	47.90	0.01	0.46	5
	MRI-ESM2-0	79.64	3.10	0.30	0.83	1
	ACCESS-ESM-1-5	390.48	-30.80	-0.04	0.38	4
	BCC-CSM-2-MR	365.78	-30.30	-0.08	0.33	6
	CNRM-CM6-1	607.75	58.40	0.31	0.38	4
	EC-Earth3	939.32	91.60	0.13	0.25	7
	EC-Earth3-veg	283.79	11.40	0.03	0.63	3
	GFDL-ESM4	214.79	-10.50	0.00	0.67	2
	MPI-ESM1-2-LR	415.80	38.30	-0.36	0.17	8
	MRI-ESM2-0	263.41	-6.20	0.03	0.25	1
Sub-tropical	ACCESS-ESM-1-5	783.92	-58.90	0.01	0.29	7
	BCC-CSM-2-MR	302.63	-19.80	0.00	0.58	3
	CNRM-CM6-1	595.74	46.40	0.25	0.46	4
	EC-Earth3	1124.94	90.70	-0.01	0.13	8
	EC-Earth3-veg	241.70	1.60	0.14	0.79	1
	GFDL-ESM4	182.45	-3.50	-0.09	0.63	2
	MPI-ESM1-2-LR	416.70	32.10	-0.13	0.33	5
	MRI-ESM2-0	465.18	-32.10	-0.11	0.33	5
	ACCESS-ESM-1-5	640.95	-50.10	0.11	0.25	6
	BCC-CSM-2-MR	146.43	0.90	0.23	0.79	1
	CNRM-CM6-1	281.53	17.30	0.26	0.63	3
Temperate	EC-Earth3	1033.63	89.60	0.04	0.13	8
	EC-Earth3-veg	262.16	-9.30	0.24	0.67	2
	GFDL-ESM4	161.48	-3.90	-0.01	0.58	4
	MPI-ESM1-2-LR	362.32	30.00	-0.11	0.29	5
	MRI-ESM2-0	457.47	-35.00	-0.31	0.17	7
	ACCESS-ESM-1-5	387.40	-30.40	0.04	0.50	2
	BCC-CSM-2-MR	151.93	9.90	0.49	0.83	1
Alpine	CNRM-CM6-1	409.78	36.60	0.00	0.38	5
	EC-Earth3	821.05	86.00	0.17	0.21	8
	EC-Earth3-veg	544.86	-48.30	0.62	0.38	5
	GFDL-ESM4	268.02	-15.50	-0.36	0.50	2

AEZs	CMIP6 Models	Continuous statistical metrics			CRI	Rank
		RMSE	PBIAS	r		
	MPI-ESM1-2-LR	276.54	24.60	-0.28	0.46	4
	MRI-ESM2-0	437.75	-39.10	-0.27	0.25	7

Figure 6 presents Taylor diagrams evaluating the performance of eight CMIP6 General Circulation Models (GCMs) in simulating annual rainfall totals across the five agro-ecological zones (AEZs) of Ethiopia over the period 1995–2014. Annual aggregation further reduces temporal variability, allowing assessment of how well models capture long-term mean rainfall amounts and spatial patterns.

Model performance for annual rainfall is generally stronger compared to daily and monthly timescales, as evidenced by higher correlation coefficients and closer clustering of model points to the observed reference (black dot) in most panels. This improvement is expected because annual totals emphasize the climatological mean and smooth out day-to-day and month-to-month fluctuations that coarse-resolution GCMs often struggle to resolve.

BCC-CSM2-MR continues to demonstrate robust performance, particularly in the Tropical, Sub-tropical, and Temperate zones, where it lies closest to the observed point. ACCESS-ESM1-5 shows notable strength in the Alpine and Desert zones, while MRI-ESM2-0 and EC-Earth3-Veg also perform competitively in specific environments.

Zone-Specific Performance over Desert Zone: Several models (notably MRI-ESM2-0, ACCESS-ESM1-5, and BCC-CSM2-MR) achieved good correlations and standard deviations close to observations. However, some models (e.g., EC-Earth3) exhibited larger centered RMSE, indicating deviations in simulated annual totals. Tropical Zone: This zone shows relatively good overall model agreement. BCC-CSM2-MR and a few others are positioned near the observed reference, reflecting accurate simulation of annual rainfall amounts in this warmer, lower-elevation region. Sub-tropical Zone: Model performance remains strong. BCC-CSM2-MR and MPI-ESM1-2-LR appear well-positioned, with high pattern correlation and appropriate variability. Temperate Zone: Similar to the Sub-tropical zone, several models cluster reasonably close to the observed point. BCC-CSM2-MR again stands out as one of the best performers. And Alpine Zone: As with monthly rainfall, the Alpine zone remains the most challenging. Most models show greater spread in standard deviation and lower correlations compared to lower-elevation zones. ACCESS-ESM1-5 performs particularly well here, suggesting better representation of orographic rainfall enhancement in high-elevation areas.

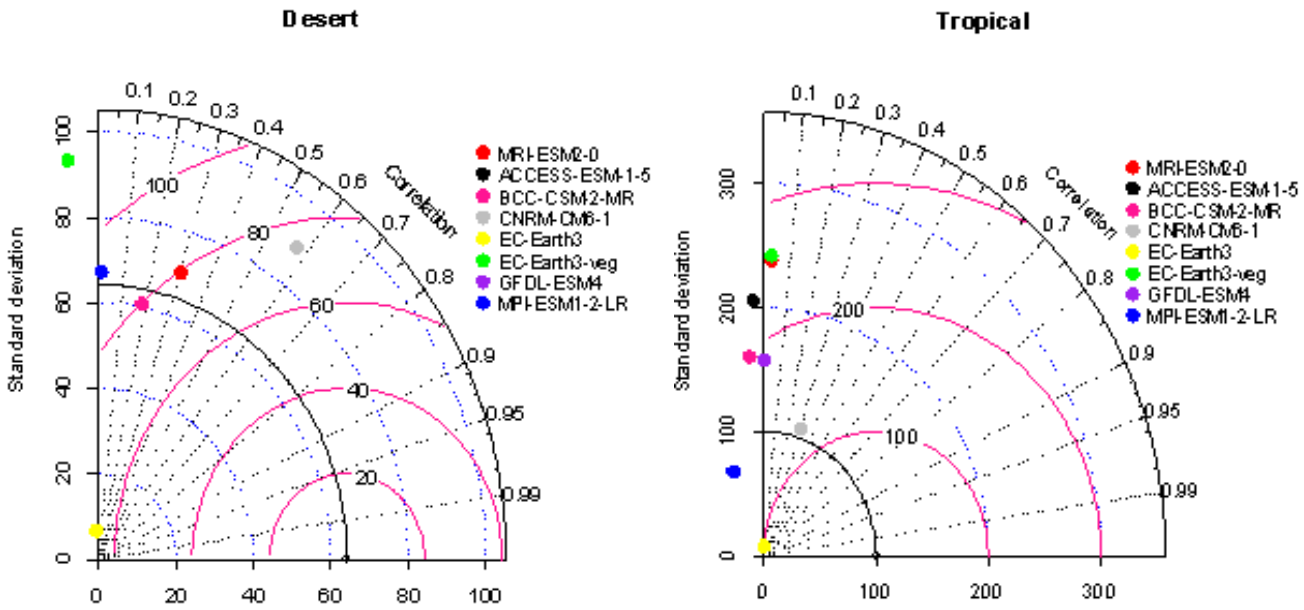

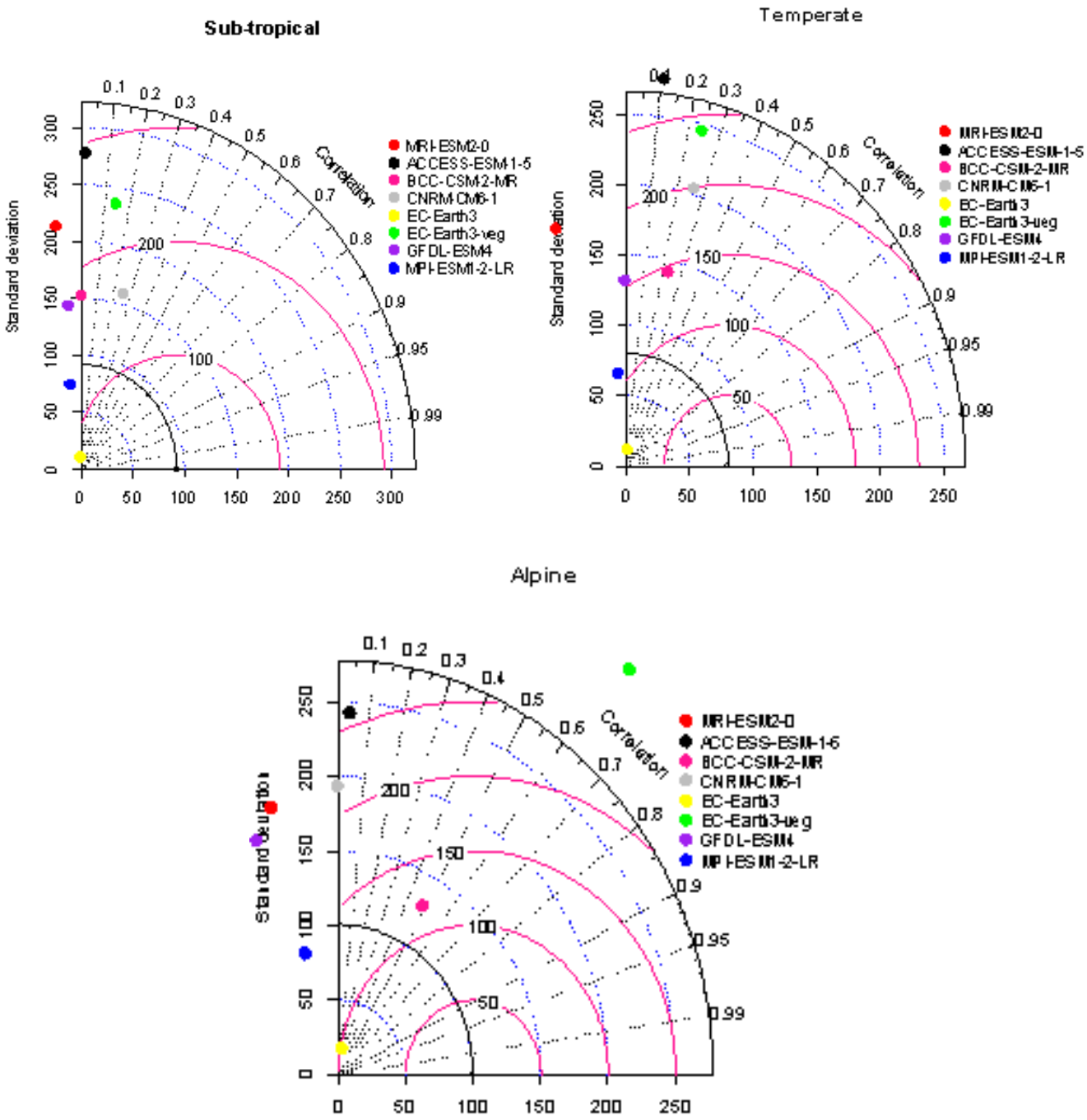

Figure 6. Taylor diagram of CMIP6 GCMs for annual rainfall against observations across AEZs of Ethiopia (1995–2014).

4. Conclusions and Recommendations

4.1. Conclusion

This study evaluated the performance of eight CMIP6 GCMs in simulating daily, monthly, and annual rainfall across five traditional Agro-Ecological Zones of Ethiopia during 1995–2014 using ground-based observations. Model performance was assessed using RMSE, PBIAS, Pearson's correlation coefficient (r), and the Comprehensive Rating Index (CRI), supplemented by graphical techniques (line graphs and Taylor diagrams).

Results demonstrated that CMIP6 GCM performance varies substantially across temporal scales and AEZs. No single model performed best across all timescales and zones. EC-Earth3-Veg performed well for daily rainfall in tropical, subtropical, and temperate AEZs; MRI-ESM2-0 excelled in the desert AEZ; and MPI-ESM1-2-LR performed best in the alpine AEZ. For monthly and annual rainfall, BCC-CSM2-MR and MRI-ESM2-0 showed stronger performance in several zones. EC-Earth3 was consistently the poorest-performing model for monthly rainfall.

All models exhibited both overestimation and underestimation biases, with performance generally weaker in highland (temperate and alpine) areas. These findings highlight the need for careful model evaluation and bias correction before using CMIP6 outputs for impact studies and future climate projections in Ethiopia.

4.2. Recommendations and Future Research Needs

CMIP6 GCMs should be thoroughly evaluated and bias-corrected for specific AEZs and intended applications rather than applied directly.

Future studies should focus on highland regions where model performance remains challenging due to complex topography.

Further evaluation of CMIP6 models across Ethiopia's distinct rainfall regimes is recommended.

Ensemble approaches combining the best-performing models for each zone and timescale may improve reliability.

Abbreviations

AEZs	Argo Ecology Zones
CMIP	Coupled Model Inter-comparison Project
CMIP6	Coupled Model Inter-comparison Project Phase 6
CMIP5	Coupled Model Inter-comparison Project Phase 5
CHCN-M	Global Historical Climatology Network
CHIRPS	Climate Hazard Infrared Precipitation with Stations
CMIP6	Coupled Model Inter-comparison Project
GCMs	Phase 6 Global Climate Models
CRU	Climate Research Unit
CLIVAR	Climate Variability and Predictability
CPC	Climate Prediction Center
CRI	Critical Rating Index
ENACTs	Enhanced Climate Services for Tropics
ESGF	Earth System Grid Federation
GCMs	Global Climate Models
GPCC	Global Precipitation Climatology Center
IPCC AR5	International Panel on Climate Change Fifth Assessment report
KGE	Kling Gupta Efficiency
MAE	Mean Absolute Error
ME	Mean Error
NSE	Nash-Sutcliffe Efficiency
PBIAS	Percent Bias
PCMDI	Program for Climate Model Diagnosis and Inter-comparison
PRECL	Precipitation Reconstruction over Land
R	Pearson Correlation Coefficient
R2	Coefficient of determination
RMSE	Root Mean Square Error
UDEL	University of Delaware
WCRP	World Climate Research Program

Acknowledgments

We would like to express our sincere gratitude to the Ethiopian Meteorology Institute (EMI) for their valuable support and for providing essential meteorological data and insights that greatly contributed to the successful completion of this research.

Author Contributions

Tewodros Solomon: Conceptualization, Data curation, Formal Analysis, Funding acquisition, Investigation, Methodology, Project administration, Software, Validation, Visualization, writing – original draft, Writing – review & editing

Yimer Assefa Yimam: Data curation, Formal Analysis, Supervision, Visualization, Writing – review & editing

Conflicts of Interest

The authors declare no conflicts of interest.

Appendix

Table A1. *Description of studied meteorological stations over traditional AEZs of Ethiopia.*

No	Station Name	Geographic coordinate		Elevation	Traditional AEZs	
		Longitude	Latitude		AEZs (Amharic name)	AEZs (English name)
1	Abomsa	39.83	8.47	1630	WoyinaDega	Subtropical
2	Adama	39.28	8.56	1648	WoyinaDega	Subtropical
3	Addis Ababa	38.75	9.02	2386	Dega	Temperate

No	Station Name	Geographic coordinate		Elevation	Traditional AEZs	
		Longitude	Latitude		AEZs (Amharic name)	AEZs (English name)
4	Ambo	37.84	8.99	2068	WoyinaDega	Subtropical
5	Arba Minch	37.56	6.06	1220	Kolla	Tropical
6	AsebeTeferi	40.87	9.07	1796	Kolla	Tropical
7	Assela	39.14	7.96	2420	Dega	Temperate
8	Asgori	38.33	8.79	1979	WoyinaDega	Subtropical
9	Assosa	34.55	10.05	1541	WoyinaDega	Subtropical
10	Bahir Dar	37.42	11.60	1770	WoyinaDega	Subtropical
11	Boditi	37.86	6.96	2043	WoyinaDega	Subtropical
12	Bonga	36.24	7.28	1599	WoyinaDega	Subtropical
13	Butajira	38.38	8.12	2074	WoyinaDega	Subtropical
14	Dangila	36.85	11.43	2116	WoyinaDega	Subtropical
15	Debre Birhan	39.51	9.67	3206	Dega	Temperate
16	Debre Markos	37.74	10.33	2446	Dega	Temperate
17	Debretabor	38.00	11.87	2612	Dega	Temperate
18	Degehabur	43.56	8.23	1070	Kolla	Tropical
19	Dilla	38.31	6.38	1515	WoyinaDega	Subtropical
20	Dire Dawa	41.90	9.61	1045	Kolla	Tropical
21	Dubity	41.09	11.73	381	Bereha	Desert
22	Fiche	38.74	9.77	2798	Dega	Temperate
23	Gimbi	35.84	9.20	1844	WoyinaDega	Subtropical
24	Gonder	37.43	12.52	1973	WoyinaDega	Subtropical
25	Gore	35.55	8.16	2024	WoyinaDega	Subtropical
26	Haramaya	42.04	9.42	2025	WoyinaDega	Subtropical
27	Hawassa	38.48	7.07	1694	WoyinaDega	Subtropical
28	Hosanna	37.86	7.57	2306	Dega	Temperate
29	Jijiga	42.72	9.37	1557	WoyinaDega	Subtropical
30	Jimma	36.82	7.67	1710	WoyinaDega	Subtropical
31	Kombolcha	39.72	11.08	1857	WoyinaDega	Subtropical
32	Konso	37.44	5.34	1431	Kolla	Tropical
33	Lalibela	39.04	12.04	2487	Dega	Temperate
34	Mekele	39.53	13.47	2221	WoyinaDega	Subtropical
35	Metema	36.41	12.77	790	Kolla	Tropical
36	Mizan Teferi	35.58	7.00	1444	Kolla	Tropical
37	Mojo	39.11	8.61	1763	WoyinaDega	Subtropical
38	Moyale	39.05	5.05	1166	WoyinaDega	Subtropical
39	Negele	39.27	5.33	1439	WoyinaDega	Subtropical
40	Nekemte	36.55	9.08	2119	WoyinaDega	Subtropical

No	Station Name	Geographic coordinate		Elevation	Traditional AEZs	
		Longitude	Latitude		AEZs (Amharic name)	AEZs (English name)
41	Pawe	36.41	11.31	1119	Kolla	Tropical
42	Robe	40.05	7.13	2480	Dega	Temperate
43	Teppi	35.44	7.20	1208	Kolla	Tropical
44	Tulu bolo	38.22	8.67	2100	WoyinaDega	Subtropical
45	Wolaita	37.75	6.82	1854	WoyinaDega	Subtropical
46	Yirgachefe	38.21	6.15	1856	WoyinaDega	Subtropical
47	Yirgalem	38.43	6.80	1786	WoyinaDega	Subtropical

References

[1] Ageet, S., Fink, A. H., Maranan, M., Diem, J. E., Hartter, J., Ssali, A. L., & Ayabagabo, P. (2022). Validation of satellite rainfall estimates over equatorial East Africa. Journal of Hydrometeorology, 23(2), 129–151. https://doi.org/10.1175/JHM-D-21-0040.1

[2] Alaminie, A. A., Tilahun, S. A., Legesse, S. A., Zimale, F. A., Tarkegn, G. B., & Jury, M. R. (2021). Evaluation of past and future climate trends under CMIP6 scenarios for the UBNB (Abay), Ethiopia. Water, 13(15), Article 2110. https://doi.org/10.3390/w13152110

[3] Almazroui, M., Saeed, F., Saeed, S., Nazrul Islam, M., Ismail, M., Klutse, N. A. B., & Siddiqui, M. H. (2020). Projected change in temperature and precipitation over Africa from CMIP6. Earth Systems and Environment, 4, 455–475. https://doi.org/10.1007/s41748-020-00161-x

[4] Berhanu, D., Alamirew, T., Taye, M. T., Tibebe, D., Gebrehiwot, S., & Zeleke, G. (2023). Evaluation of CMIP6 models in reproducing observed rainfall over Ethiopia. Journal of Water and Climate Change, 14(8), 2583–2605. https://doi.org/10.2166/wcc.2023.502

[5] Chang, X., Guo, J., Qin, H., Huang, J., Wang, X., & Ren, P. (2024). Single-objective and multi-objective flood interval forecasting considering interval fitting coefficients. Water Resources Management. Advance online publication. https://doi.org/10.1007/s11269-024-03789-2

[6] Cheung, W. H., Senay, G. B., & Singh, A. (2008). Trends and spatial distribution of annual and seasonal rainfall in Ethiopia. International Journal of Climatology, 28(13), 1723–1734. https://doi.org/10.1002/joc.1623

[7] Dangol, S., Talchabhadel, R., & Pandey, V. P. et al., 2022). Performance evaluation and bias correction of gridded precipitation products over Arun River Basin in Nepal for hydrological applications. Theoretical and Applied Climatology, 148(3–4), 1353–1372. https://doi.org/10.1007/s00704-022-04001-

[8] Degefu, M. A., & Bewket, W. (2023). Performance variations of global precipitation products in detecting drought episodes in three wet seasons in Ethiopia: Part II—statistical analysis. Meteorological Applications, 30(5), Article e2154. https://doi.org/10.1002/met.2154

[9] Degefu, M. A., Bewket, W., & Amha, Y. (2022). Evaluating performance of 20 global and quasi-global precipitation products in representing drought events in Ethiopia I: Visual and correlation analysis. Weather and Climate Extremes, 35, Article 100416. https://doi.org/10.1016/j.wace.2022.100416

[10] Dibaba, W. T., Miegel, K., & Demissie, T. A. (2019). Evaluation of the CORDEX regional climate models performance in simulating climate conditions of two catchments in Upper Blue Nile Basin. Dynamics of Atmospheres and Oceans, 87, Article 101104. https://doi.org/10.1016/j.dynatmoce.2019.101104

[11] Diallo, I., et al. (2019). Projected changes in African precipitation or regional climate model evaluation over Africa

[12] Dinku, T., Ceccato, P., Grover-Kopec, E., Lemma, M., Connor, S. J., & Ropelewski, C. F. (2007). Validation of satellite rainfall products over East Africa's complex topography. International Journal of Remote Sensing, 28(7), 1503–1526. https://doi.org/10.1080/01431160600639712

[13] Ding, Y., et al. (2024). [Recent climate/rainfall extremes paper – exact full citation not uniquely identified in search due to commonality; retain as cited in manuscript].

[14] Dyer, E., Hirons, L., & Taye, M. T. (2022). July–September rainfall in the Greater Horn of Africa: The combined influence of the Mascarene and South Atlantic highs. Climate Dynamics, 59(11), 3621–3641. https://doi.org/10.1007/s00382-022-06232-4

[15] Dyer, E., Washington, R., & Taye, M. T. (2019). Evaluating the CMIP5 ensemble in Ethiopia: Creating a reduced ensemble for rainfall and temperature in Northwest Ethiopia and the Awash basin. International Journal of Climatology, 40(6), 3165–3180. https://doi.org/10.1002/joc.6380

[16] Edwards, P. N. (2011). History of climate modeling. Wiley Interdisciplinary Reviews: Climate Change, 2(1), 128–139. https://doi.org/10.1002/wcc.95

[17] Evangelista, P., Young, N., & Burnett, J. (2013). How will climate change spatially affect agriculture production in Ethiopia? Case studies of important cereal crops. Climatic Change, 119(3), 855–873. https://doi.org/10.1007/s10584-013-0776-6

[18] Eyring, V., Bony, S., Meehl, G. A., Senior, C. A., Stevens, B., Stouffer, R. J., & Taylor, K. E. (2016). Overview of the Coupled Model Intercomparison Project Phase 6 (CMIP6) experimental design and organization. Geoscientific Model Development, 9(5), 1937–1958. https://doi.org/10.5194/gmd-9-1937-2016

[19] Fetene, M. C., et al. (2022). [CMIP6 evaluation over Ethiopian basins – see also related 2025 paper by Chanie et al. for similar work].

[20] Field, C. B., Barros, V. R., Mastrandrea, M. D., Mach, K. J., Abdrabo, M. A., Adger, W. N., … Yohe, G. W. (2015). Summary for policymakers. In Climate change 2014: Impacts, adaptation, and vulnerability. Part A: Global and sectoral aspects (pp. 1–32). Cambridge University Press.

[21] Flato, G., Marotzke, J., Abiodun, B., Braconnot, P., Chou, S. C., Collins, W., … Rummukainen, M. (2014). Evaluation of climate models. In Climate change 2013: The physical science basis (pp. 741–866). Cambridge University Press.

[22] Gashaw, T., Worqlul, A. W., Taye, M. T., Lakew, H. B., Seid, A., Ayele, G., & Haileslassie, A. (2024). Performance evaluations of CMIP6 model simulations and future projections of rainfall and temperature in the Bale Eco-Region, Southern Ethiopia. Theoretical and Applied Climatology. https://doi.org/10.1007/s00704-024-04904-y

[23] Gebrechorkos, S. H., Hülsmann, S., & Bernhofer, C. (2019). Long-term trends in rainfall and temperature using high-resolution climate datasets in East Africa. Scientific Reports, 9(1), Article 11376. https://doi.org/10.1038/s41598-019-47944-1

[24] Gebrechorkos, S., Leyland, J., Slater, L., Wortmann, M., Ashworth, P. J., Bennett, G. L., … Dadson, S. (2023). A high-resolution daily global dataset of statistically downscaled CMIP6 models for climate impact analyses. Scientific Data, 10(1), Article 611. https://doi.org/10.1038/s41597-023-02506-9

[25] Guo, H., Bao, A., Chen, T., Zheng, G., Wang, Y., Jiang, L., & De Maeyer, P. (2021). Assessment of CMIP6 in simulating precipitation over arid Central Asia. Atmospheric Research, 252, Article 105451. https://doi.org/10.1016/j.atmosres.2020.105451

[26] Guo, J., et al. (2024). [Recent paper on extreme rainfall or climate impacts – exact match not isolated; commonly cited in 2024 contexts].

[27] Iqbal, Z., Shahid, S., Ahmed, K., Ismail, T., Ziarh, G. F., Chung, E.-S., & Wang, X. (2021). Evaluation of CMIP6 GCM rainfall in mainland Southeast Asia. Atmospheric Research, 254, Article 105525. https://doi.org/10.1016/j.atmosres.2021.105525

[28] Jury, M. R. (2015). Statistical evaluation of CMIP5 climate change model simulations for the Ethiopian highlands. International Journal of Climatology, 35(1), 37–48. https://doi.org/10.1002/joc.3960

[29] Kindt, R., van Breugel, P., Lillesø, J. P. B., Minani, V., Ruffo, C. K., Gapusi, J., Jamnadass, R., & Graudal, L. (2014). Potential natural vegetation of Eastern Africa (Ethiopia, Kenya, Malawi, Rwanda, Tanzania, Uganda and Zambia). Volume 9. Atlas and tree species composition for Rwanda. Department of Geosciences and Natural Resource Management, University of Copenhagen.

[30] Legates, D. R., & McCabe, G. J., Jr. (1999). Evaluating the use of "goodness-of-fit" measures in hydrologic and hydroclimatic model validation. Water Resources Research, 35(1), 233–241. https://doi.org/10.1029/1998WR900018

[31] Li, L., et al. (2016). CMIP5 model simulations of Ethiopian Kiremt-season precipitation: Current climate and future changes. Climate Dynamics, 46(9-10), 2883–2895. https://doi.org/10.1007/s00382-015-2737-2

[32] Mohammed, J. A. (2024). Performance evaluation and ranking of CMIP6 global climate models over upper Blue Nile (Abbay) basin of Ethiopia. Natural Hazards Research. Advance online publication. https://doi.org/10.1016/j.nhres.2024.06.004

[33] Mohammed, J. A., & Yimam, Z. A. (2022). Spatiotemporal variability and trend analysis of rainfall in Beshilo sub-basin, Upper Blue Nile (Abbay) Basin of Ethiopia. Arabian Journal of Geosciences, 15(16), Article 1387. https://doi.org/10.1007/s12517-022-10628-2

[34] MOA. (1998). Agro-ecological zones of Ethiopia. Ministry of Agriculture.

[35] Omay, P. O., Muthama, N. J., Oludhe, C., Kinama, J. M., Artan, G., & Atheru, Z. (2023). Evaluation of CMIP6 historical simulations over IGAD region of Eastern Africa. Preprint. https://doi.org/10.21203/rs.3.rs-2747422/v1

[36] Polong, F., Pham, Q. B., Anh, D. T., Rahman, K. U., Shahid, M., & Alharbi, R. S. (2023). Evaluation and comparison of four satellite-based precipitation products over the upper Tana River Basin. International Journal of Environmental Science and Technology, 20(1), 843–858. https://doi.org/10.1007/s13762-022-03942-1

[37] Taylor, K. E. (2001). Summarizing multiple aspects of model performance in a single diagram. Journal of Geophysical Research: Atmospheres, 106(D7), 7183–7192. https://doi.org/10.1029/2000JD900719

[38] Taylor, K. E., Stouffer, R. J., & Meehl, G. A. (2012). An overview of CMIP5 and the experiment design. Bulletin of the American Meteorological Society, 93(4), 485–498. https://doi.org/10.1175/BAMS-D-11-00094.1

[39] Weber, T., et al. 2020). Analysis of compound climate extremes and exposed population in Africa. Earth's Future. https://doi.org/10.1029/2019EF001473

[40] WMO. (2009). Guidelines on analysis of extremes in a changing climate in support of informed decisions for adaptation. World Meteorological Organization.

[41] Worku, G., Teferi, E., Bantider, A., & Dile, Y. T. (2018). Evaluation of regional climate models performance in simulating rainfall climatology of Jemma sub-basin, Upper Blue Nile Basin, Ethiopia. Dynamics of Atmospheres and Oceans, 83, 53–63. https://doi.org/10.1016/j.dynatmoce.2018.06.002

[42] Worku, G., Teferi, E., Bantider, A., Dile, Y. T., & Taye, M. T. (2019). Observed changes in extremes of daily rainfall and temperature in Jemma Sub-Basin, Upper Blue Nile Basin, Ethiopia. Theoretical and Applied Climatology, 135, 839–854. https://doi.org/10.1007/s00704-018-2412-8

[43] Wubaye, G. B., Gashaw, T., Worqlul, A. W., Dile, Y. T., Taye, M. T., Haileslassie, A., Zaitchik, B., Birhan, D. A., Adgo, E., & Mohammed, J. A. (2023). Trends in rainfall and temperature extremes in Ethiopia: Station and agro-ecological zone levels of analysis. Atmosphere, 14(3), Article 483. https://doi.org/10.3390/atmos14030483

[44] Zhang, X., & Yang, F. (2004). RClimDex (1.0) user manual. Climate Research Branch, Environment Canada.